

Intermittent Sampling in Iterative Learning Control: a Monotonically-Convergent Gradient-Descent Approach with Application to Time Stamping

Nard Strijbosch, Tom Oomen

Abstract—The standard assumption that a measurement signal is available at each sample in iterative learning control (ILC) is not always justified, e.g., in systems with data dropouts or when exploiting time-stamped data from incremental encoders. The aim of this paper is to develop a computationally tractable ILC framework for systems with arbitrary time-varying measurement points. New conditions for monotonic convergence of the input signal are established. These lead to a new single centralized design approach independent of the sampling times reminiscent of gradient-descent ILC. The approach is demonstrated in a simulation example of a mass-spring-damper system from which exact time-varying time-stamped data from the incremental encoder is available.

I. INTRODUCTION

Iterative learning control (ILC) can achieve high performance for systems that perform repetitive tasks [1], [2]. The key idea of ILC is to iteratively determine an input signal that compensates for the reproducible part of the error, by learning from the error signal observed during previous iterations of the same task.

Typical ILC design approaches that have been successfully implemented have favourable properties including 1) an explicit learning update, instead of performing an optimization at each iteration, see [3] for details, 2) achieving monotonic convergence in an appropriate norm of either the sequence of control inputs or the sequence of error signals [4]. Several approaches addressing these aspects: approaches based on frequency response measurement data, see e.g., [5], [6], norm optimal based approaches, see e.g., [7], [8], and the robust gradient-descent based ILC approach, see e.g., [9], [10]. These design frameworks typically lead to explicit filters, either linear time-invariant (LTI) or linear time-varying (LTV), and have been successfully implemented in standard digital control implementations.

An important example where standard ILC assumptions are not justified is when time-stamped data from incremental encoders is exploited [11]. This data is non-equidistant and generally in between sample instances, therefore, violating the assumption of the availability of an exact measurement at the sample instances. This assumption is also violated in intermittent ILC through data dropouts in networks [12], [13], stealth attacks [14], or other constraints [15], [16].

Nard Strijbosch and Tom Oomen are with the Control Systems Technology Group, Department of Mechanical Engineering, Eindhoven University of Technology, P.O. Box 513, 5600 MB Eindhoven, The Netherlands, e-mail: n.w.a.strijbosch@tue.nl, t.a.e.oomen@tue.nl. This work is part of the research programme VIDI with project number 15698, which is (partly) financed by the Netherlands Organisation for Scientific Research (NWO).

Intermittent observations occur due to various (cyber-)physical phenomena, which have led to several modelling approaches, see e.g., [12], [13], [16]. These approaches assume that the availability of data at each possible time instant is given by a known probability distribution, leading to convergence results for the expected available data. This probability distribution is unknown in many applications. Consider for instance time-stamped data from incremental encoders where the availability of data at each time instant is strongly related to the position which cannot be modelled by a probability distribution. A worst-case analysis, thereby omitting the necessity of modelling the availability of data, is introduced in [11]. However, as mentioned in Remark IV.2 of [11], this approach is not computationally tractable for long trial lengths.

Although several ILC approaches that consider arbitrary time-varying measurements have been developed, guaranteed monotonic convergence has not been fully addressed and computation time aggregates. The aim of this paper is to design a single centralized controller that allows for guaranteed monotonic convergence of the input signal when only limited error information is available at arbitrary time-varying measurement points. The developed ILC algorithm extends existing intermittent ILC approaches with 1) the possibility of modelling intersample data points and 2) a worst-case analysis approach. This allows to design an ILC algorithm that exploits time-stamped data from incremental encoders for large-scale situations.

The main contribution of this paper is a computationally efficient ILC algorithm that guarantees monotonic convergence of the input signal when only limited error information is available at arbitrary time-varying measurement points. This is achieved through the following sub-contributions:

- C1 A worst-case analysis reveals intermittent sampling in ILC is not monotonically convergent in the classical sense. A new monotonic convergence definition is introduced for intermittent sampled ILC (Section III).
- C2 An intermittent sampled ILC framework is developed that leads to monotonic convergence of the control input exploiting a single decentralized controller (Section IV).
- C3 A connection is established between the developed ILC approach and the existing gradient-descent ILC design methods [9], [10]. This connection allows for an intuitive ILC design (Section V).
- C4 The ILC approach is applied to a mass-spring-damper system from which exact time-varying time-stamped data from the incremental encoder is available. These results confirm monotonic convergence (Section VI).

Proofs will be published elsewhere.

A. Notations and Definitions

The p -norm of a vector x is given by $\|x\|_p := (\sum_{i=1}^n |x_i|^p)^{\frac{1}{p}}$ where $x \in \mathbb{R}^n$ is given by $x := [x_1, x_2, \dots, x_n]^T$. The induced p norm of matrix $A \in \mathbb{R}^{n \times n}$ is defined as $\|A\|_p = \max_{w \neq 0} \frac{\|Aw\|_p}{\|w\|_p}$.

Throughout, $t \in \mathbb{Z}$ and $t_c \in \mathbb{R}$ denote discrete-time and continuous-time respectively. In block diagrams, continuous-time signals are represented by solid lines, slow sampled discrete-time signals are represented by dashed lines and fast sampled discrete-time signals are represented by dotted lines. All systems are assumed to be single-input single-output, finite-dimensional and linear time invariant (LTI).

Definition 1 (Monotonic convergence towards a fixed point.) A sequence $\{Y_i\}_{i \in \mathbb{Z}_{\geq 0}}$, $Y_i \in X$ is said to converge monotonically, in a p -norm, $p \in \{1, 2, \dots\}$, to a unique fixed point $Y_\infty \in X$, if there exists a $\kappa \in [0, 1)$ such that

$$\|Y_{j+1} - Y_\infty\|_p \leq \kappa \|Y_j - Y_\infty\|_p \quad (1)$$

is satisfied for all $Y_j \in X$, $j \in \mathbb{Z}_{\geq 0}$.

II. PROBLEM FORMULATION

In this section, the intermittent sampled ILC framework is introduced. First, the ILC setup is introduced. Several application examples including incremental encoders with time-stamped data are shown to fit this formulation. Finally, the intermittent sampled ILC problem is formulated.

A. ILC setup

Consider the ILC setup depicted in Fig. 1, where

$$y_j(t_c) = J u_j(t_c), \quad (2)$$

here J denotes a causal and stable continuous-time system, which can be either an open-loop or closed-loop system. The index $j \in \mathbb{Z}_{\geq 0}$ denotes the j -th task with a finite length of $N_l \in \mathbb{N}$ control input samples. The ideal zero-order-hold \mathcal{H}_l , with sampling time $h_l \in \mathbb{R}_{>0}$, connects the digital control input $u^l(t)$ to the analog input of J , as follows

$$\mathcal{H}_l : u_j^l(t) \mapsto u_j(t_c), \quad u_j(kh_l + \tau) = u_j^l(k), \quad (3)$$

with $\tau \in [0, h_l)$, $k \in t$. The sampled output y_j^h is obtained from the ideal sampler \mathcal{S}_h

$$\mathcal{S}_h : y_j(t_c) \mapsto y_j^h(t), \quad y_j^h(k) = y_j(h_h k), \quad k \in t \quad (4)$$

where $h_h = \frac{1}{M} h_l$, $M \in \mathbb{N}$ the sampling time of the output.

The output y^h is available to the controller only at the time-stamps $\bar{\tau}_j$, i.e., $\bar{y}_j(k) = y_j^h(\bar{t}_{j,k})$, $k \in \{1, \dots, N_{\bar{\tau}_j}\}$. Each trial, the time stamp generator TS generates, depending on the application, the sequence of time stamps $\bar{\tau}_j :=$

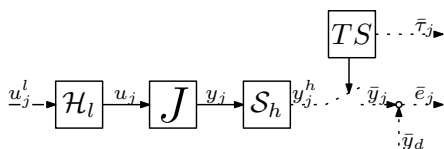


Fig. 1. Intermittent sampled ILC setup

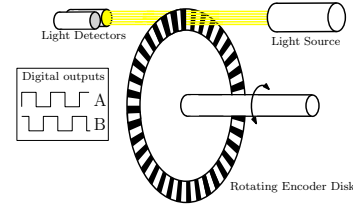


Fig. 2. Schematic representation of incremental encoder

$(\bar{t}_{j,1}, \bar{t}_{j,2}, \dots, \bar{t}_{j, N_{\bar{\tau}_j}})$ with $N_{\bar{\tau}_j} \in \{0, 1, 2, \dots, N_h\}$ the number of time stamps in the j -th trial. The desired position at the sample times of the ideal sampler \mathcal{S}_h is denoted by y_d^h . As the output is only available at the time-stamps $\bar{\tau}_j$ the error between the output y^h and the desired output y_d^h can only be defined at the time-stamps, this error is given by

$$\bar{e}_j(k) = y_d^h(\bar{t}_{j,k}) - y_j^h(\bar{t}_{j,k}), \quad k \in \{1, \dots, N_{\bar{\tau}_j}\}. \quad (5)$$

The goal of ILC is to minimize the error e^h . To achieve this the available error \bar{e}_j in task j is exploited to construct u_{j+1}^l for task $j+1$, i.e., $u_{j+1}^l = F(u_j^l, \bar{e}_j)$.

Remark 2 Note that the standard ILC setup [1] is recovered, when $\mathcal{T} = \{\bar{\tau}_0\}$, with $\bar{\tau}_0$ representing the set of time-stamps corresponding to the sample times of the control input, i.e., $\bar{\tau}_0 = (0, h_l, 2h_l, \dots, (N_l - 1)h_l)$.

B. Applications

The following applications fit in the ILC setup of Fig. 1:

- Networked systems where communication is disturbed through data dropouts, see e.g., [12], [13].
- Systems vulnerable to stealth attacks, see e.g., [14].
- Systems that exploit incremental encoders to measure position, see e.g., [11].

Systems vulnerable to data dropouts or stealth attacks fit naturally in the ILC setup given in Fig. 1, as the operator TS decides which data points are available. Monotonic convergence of these applications can be guaranteed through a worst-case analysis of the ILC setup.

To illustrate how systems that exploit incremental encoders fit the ILC setup of Fig. 1, the mechanical working principle of an incremental encoder is elaborated.

In Fig. 2, a schematic overview is presented of an incremental encoder. The main components are a slotted disk or strip in linear optical incremental encoders, a light source and two light detectors. The light source is aimed at the light detectors. Depending on the position of the encoder disk the slots either obstruct the light or allow the light through. The output of the light detectors are two signals (A,B) which indicate if the light is perceived or not by the light detector.

The digital signals (A,B) are evaluated at a very high sampling rate, f_h , ($\mathcal{O}(f_h) = 10^6 - 10^8$ Hz) and it is determined if one of the signals changed, i.e. if a line transition occurred in-between two time-instances. A counter keeps track of the number of line transitions taking the direction into account. Due to the high sampling rate f_h of the encoder, the error at the time-stamps \bar{t}_i can be neglected, i.e., $|y(\bar{t}_i) - \bar{y}(\bar{t}_i)| = 0$, as exemplified in Fig. 3.

There are several ways to exploit the data from encoders:

- The counter value at the sampling instances of the feedback system is exploited by the ILC algorithm.

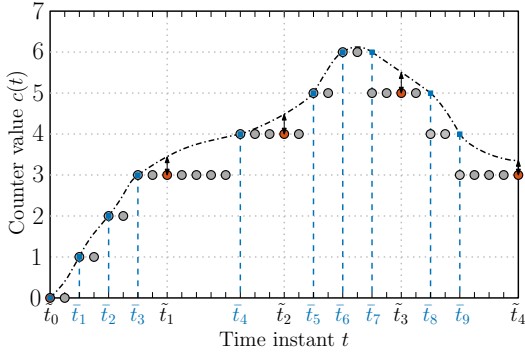


Fig. 3. The Counter value of and incremental encoder corresponding to the position indicated by (---) The encoder operates at a very high equidistant sampling rate, indicated by the circles. While the feedback control system operates at a lower equidistant sampling rate (●). Line-transitions are indicated by blue squares (■) and corresponding time-stamps \bar{t}_i . These are exact, i.e., not subject to quantization error. In contrast, data points used by the feedback control system, clearly suffer from quantization, indicated by (↔).

As the sampling frequency of the feedback controller is limited by the real-time computations this approach leads to a quantization effect. The quantization effect can be considered as an extra trial varying noise term which is amplified by ILC [3], [8].

- The offline computations in ILC facilitate the employment of the data at the time stamps, not corrupted by quantization, to obtain an increase in performance [11].

The ILC setup as depicted in Fig. 1 encompasses the ILC setup that exploits time-stamped data from incremental encoders by taking the sampling frequency of the ideal sampler (4) equal to the sampling frequency of the encoder and by defining the operator TS to define the time stamps based on the line-transitions.

C. Problem Formulation

The aim of this paper is to develop an ILC approach that guarantees monotonic convergence for ILC setups with arbitrary time-varying measurement data. This includes

- An investigation of a new notion of monotonic convergence, since existing measures do not apply (Section III).
- A derivation of conditions for a centralized ILC approach independent of the size of \mathcal{T} .
- Establishing a connection with an existing ILC approach to obtain intuitive design guidelines.

III. MONOTONIC CONVERGENCE

The effect of the control input is not fully observable in trials with few measurement points. In this section, it is shown that for these trials monotonic convergence as in Definition 1 cannot be achieved. Therefore, a new definition of monotonic convergence is introduced.

A. Assumptions

The following assumptions are imposed.

Assumption 3 For the desired output y_d^h that is considered there exists a input signal u_d^h such that $y_d^h = S_h J \mathcal{H}_l u_d^h$.

Assumption 4 The set \mathcal{T} consists of all sequences of observations possible for a data set of length N_h .

Assumption 3 ensures that it is possible to design an ILC algorithm that leads to convergence of the input signal u_j^l towards u_d^l for $j \rightarrow \infty$ and thereby achieving $e_j^h = 0$ [1]. Assumption 4 leads to a worst-case analysis for every ILC setup where the set of possible sequences of time-stamps is a subset of \mathcal{T} . Note that the size of \mathcal{T} is given by 2^{N_h} and therefore grows exponentially with respect to the trial length.

B. Finite Time Description

First, the finite-time system description of the ILC setup of Fig. 1 is introduced, to define input observability. Consider the system $J^{h,h} = S_h J \mathcal{H}_h$ with Markov parameters m_k^h , operating over a finite time interval $k \in [0, N_h] \subseteq t$, where the state of the system is reset to zero after each trial. The input-output behaviour is represented by its convolution matrix $\underline{J}^{h,h} \in \mathbb{R}^{N_h \times N_h}$ which maps the input vector $\underline{u}^h \in \mathbb{R}^{N_h}$ to the output vector $\underline{y}^h \in \mathbb{R}^{N_h}$ [17], [18]:

$$\underline{y}^h = \underline{J}^{h,h} \underline{u}^h, \quad \underline{J}^{h,h} = \begin{bmatrix} m_0^h & & 0 \\ \vdots & \ddots & \\ m_{N_h-1}^h & \dots & m_0^h \end{bmatrix} \quad (6)$$

Define the finite-time description of the zero order hold $\mathcal{H}_{h,l}$ as $\mathcal{H}_h = I_M \otimes \mathbb{I}_M$ with $\mathbb{I}_M := [1 \dots 1]^T \in \mathbb{R}^M$ and \otimes denotes the Kronecker product [19]. From this, the finite-time description of $J^{h,l} = S_h J \mathcal{H}_l$ is given by $\underline{J}^{h,l} = \underline{J}^{h,h} \mathcal{H}_{h,l}$.

Moreover, define for all $\bar{\tau} \in \mathcal{T}$, a matrix $\underline{T}_{\bar{\tau}} \in \mathbb{R}^{N_{\bar{\tau}} \times N_h}$, that maps the error vector $\underline{e}^h \in \mathbb{R}^{N_h}$ to the error vector at the corresponding time-stamps $\underline{\bar{e}}(\bar{\tau}) \in \mathbb{R}^{N_{\bar{\tau}}}$, i.e.,

$$\underline{\bar{e}}(\bar{\tau}_j) = \underline{T}_{\bar{\tau}_j} \underline{e}^h, \quad \underline{T}_{\bar{\tau}_j} = \begin{bmatrix} \epsilon_{\bar{t}_{j,1}}^T & \epsilon_{\bar{t}_{j,2}}^T & \dots & \epsilon_{\bar{t}_{j,N_{\bar{\tau}_j}}^T} \end{bmatrix}^T \quad (7)$$

where $\epsilon_k, k \in \mathbb{Z}_{\geq 0}$ is a row vector of length N_h with 1 in the k -th position and 0 in every other position.

The structure of the ILC controller is given by

$$\underline{u}_{j+1} = \underline{u}_j^l + \underline{L}_{\bar{\tau}_j} \underline{\bar{e}}_j^h \quad (8)$$

with matrices $\underline{L}_{\bar{\tau}} \in \mathbb{R}^{N_l \times N_{\bar{\tau}}}, \forall \bar{\tau} \in \mathcal{T}$.

Using these definitions the finite-time description of the intermittent ILC setup is given by

$$\begin{aligned} \underline{u}_{j+1}^l &= \underline{u}_j^l + \underline{L}_{\bar{\tau}_j} \underline{T}_{\bar{\tau}_j} \underline{e}_j^h, \\ \underline{e}_j^h &= \underline{y}_j^h - \underline{J}^{h,l} \underline{u}_j^l, \\ \bar{\tau}_j &\in \mathcal{T}. \end{aligned} \quad (9)$$

C. Input observability in ILC

There exist sequences with few measurement points in the set \mathcal{T} . For some of these sequences, the control input is not fully observable in the available error, $\underline{\bar{e}}$. Due, to the iteration varying measurement points this leads to varying observability of the input signal. Analogous to the well-known system theoretic results, e.g., [20, Section 5.3], the input observability of the ILC setup (9) is defined as follows.

Definition 5 (Input Observability) Consider the finite time ILC description (9) at a given iteration j with corresponding sequence of measurement points $\bar{\tau}_j \in \mathcal{T}$. The input $u_j^l \in \mathbb{R}^{N_l}$ is called observable from the output \bar{y}_j of iteration j if \bar{y}_j together with the laws of the system, determines u_j^l uniquely. This implies that if the input u_j^l

is observable from \bar{y}_j that there exist for each output $\bar{y}_j \in \mathbb{R}^{N_{\bar{\tau}_j}}$ at most one input u_j^l such that $\bar{y}_j = T_{\bar{\tau}_j} J^{h,l} u_j^l$.

From Definition 5 the following partitioning of the input in an observable and unobservable part can be obtained.

Theorem 6 Consider the finite time ILC description (9) and a sequence of measurement points $\bar{\tau}_j \in \mathcal{T}$. If the input u_j^l is not observable as in Definition 5, then there exists a transformation of the input given by

$$u_j^l = u_{j, \text{obj}}^l + u_{j, \text{uoj}}^l = S_{1\bar{\tau}_j} u_{j,1}^l + S_{2\bar{\tau}_j} u_{j,2}^l \quad (10)$$

with $S_{\bar{\tau}_j} = [S_{1,\bar{\tau}_j} \quad S_{2,\bar{\tau}_j}]$ a nonsingular matrix, such that the input $u_{j, \text{obj}}^l := S_{1\bar{\tau}_j} u_{j,1}^l$ is observable in the output and \bar{y}_j , and the input $u_{j, \text{uoj}}^l := S_{2\bar{\tau}_j} u_{j,2}^l$ is not observable in the output \bar{y}_j .

D. Monotonic convergence of intermittent sampled ILC

In this section it is shown that monotonic convergence of the sequence of inputs $\{u_j^l\}_{j \in \mathbb{N}}$ as in Definition 1 cannot be achieved when the control input is not observable as in Definition 5. Based on the transformation of the control input in an observable and unobservable part, a new definition of monotonic convergence is introduced.

To illustrate that input observability is necessary to achieve monotonic convergence of the control input as in Definition 1, the trial invariant ILC system for which the input is not observable is considered, leading to the following result.

Theorem 7 Consider an ILC setup (9) satisfying Assumption 3 with trial invariant sequence of measurement points, i.e., $\tau_j = \bar{\tau}$ with $\bar{\tau} \in \mathcal{T}$. If the control input u_j^l is not fully observable, as in Definition 5, then there does not exist a matrix $\underline{L}_{\bar{\tau}} \in \mathbb{R}^{N_l \times N_{\bar{\tau}}}$ that guarantees monotonic convergence in any p -norm of the sequence of input signals $\{u_j^l\}_{j \in \mathbb{Z}_{>0}}$, as in Definition 1.

As a consequence of Theorem 7, monotonic convergence of the sequence of input signals as in Definition 1 cannot be guaranteed for the ILC setup with arbitrary time-varying measurement points through a worst-case analysis, leading to contribution C1. To allow a proper study of the ILC setup, the following definition of monotonic convergence of the control input is introduced.

Definition 8 (Monotonic convergence with trial varying input observability) The sequence of input signals $\{u_j^l\}_{j \in \mathbb{Z}_{>0}}$ of the ILC setup with arbitrary time-varying measurement points is called monotonic convergent in a given p -norm if there exists a $\kappa_{\text{ob}} \in [0, 1)$ such that p -norm of the observable part of the input during trial j converges monotone towards the corresponding part of u_d^l , i.e.,

$$\|u_{j+1, \text{obj}}^l - u_{d, \text{obj}}^l\|_p \leq \kappa_{\text{ob}} \|u_{j, \text{obj}}^l - u_{d, \text{obj}}^l\|_p \quad (11)$$

where $u_{j, \text{obj}}^l$ is the observable part of input u_j^l corresponding to the transformation (10). In addition, the following should be satisfied for some $\kappa_{\text{tot}} \in [0, 1]$

$$\|u_{j+1}^l - u_{\infty}^l\|_p \leq \kappa_{\text{tot}} \|u_j^l - u_{\infty}^l\|_p. \quad (12)$$

to guarantee that the unobservable part of the control input is monotone non-decreasing.

Remark 9 Definition 8 reduces to the monotonic convergence condition (1) when considering an ILC setup where the input is fully observable in each trial.

Condition (11) states that the observable part $u_{j, \text{obj}}^l$ of the j -th trial should converge monotonically towards the corresponding fixed point $u_{\infty, \text{obj}}^l$. By definition, this part of the control input is fully observable in the available output of the j -th trial, therefore based on the available information the control input for trial $j+1$ in the transformation of trial j , i.e., $u_{j+1, \text{obj}}^l$ can be constructed to converge monotonically as in Definition 1. When considering an iteration invariant ILC setup, the analysis of the observable part of the input, is equivalent to the ILC approach introduced in [21].

In iteration invariant ILC setups the unobservable input space does not change, therefore $u_{d, \text{uoj}}^l = 0$ can be obtained by altering (8) such that $\|u_{j+1, \text{uoj}}^l\|_p = \alpha \|u_{j, \text{uoj}}^l\|_p$ for some $\alpha \in [0, 1)$, thereby satisfying (12) with $\kappa_{\text{tot}} \in [0, 1)$. When considering an ILC setup with iteration varying observability properties, typically $u_{d, \text{uoj}}^l \neq 0$. Therefore, applying a similar approach leads to a violation of (12), as the observable part converges towards 0 instead of $u_{d, \text{uoj}}^l \neq 0$. However, designing the ILC controller (8) such that $u_{j+1, \text{uoj}}^l = u_{j, \text{uoj}}^l$, guarantees Condition (12) if Condition (11) is satisfied.

IV. COMPUTATIONALLY TRACTABLE ILC APPROACH

In this section, a computationally tractable ILC approach is developed to design (8) for the ILC setup presented in Fig. 1. From Definition 8, a necessary structure is derived for the ILC controller to guarantee monotonic convergence in the 2-norm. This structure is exploited to develop an ILC approach that is independent of the size of \mathcal{T} .

A. Monotonic Convergence in the 2-norm

Next, for all $\bar{\tau} \in \mathcal{T}$ a structure for the corresponding matrix $\underline{L}_{\bar{\tau}}$ is derived that is necessary to achieve monotonic convergence as in Definition 8.

Theorem 10 (Monotonic convergence in the 2-norm)

Consider the finite-time time-stamped ILC system (9) satisfying Assumption 3. The sequence of control inputs $\{u_j^l\}_{j \in \mathbb{N}}$ is monotonic convergent in the 2-norm towards the fixed point u_d^l as in Definition 8, if and only for each $\bar{\tau} \in \mathcal{T}$ the corresponding matrix $\underline{L}_{\bar{\tau}}, \bar{\tau} \in \mathcal{T}$ is given by

$$\underline{L}_{\bar{\tau}} = J^T T_{\bar{\tau}}^T X_{\bar{\tau}} \quad (13)$$

with $X_{\bar{\tau}} \in \mathbb{R}^{N_{\bar{\tau}} \times N_{\bar{\tau}}}$. Moreover, if for each $\bar{\tau} \in \mathcal{T}$ a matrix $\underline{L}_{\bar{\tau}}$ of this structure is found such that Condition (11) is satisfied, Condition (12) is automatically guaranteed.

From the result of Theorem 10, it is concluded that if the matrices $\underline{L}_{\bar{\tau}}$ are of the form (13), the ILC problem reduces to finding for each $\bar{\tau} \in \mathcal{T}$ a matrix $X_{\bar{\tau}}$ such that Condition (11) is satisfied.

B. Decentralized ILC controller

Next, a centralized ILC framework for the ILC setup (9) is developed that reduces the design problem to finding a single matrix \underline{L} , leading to Contribution C2 of this paper.

The following structure of the centralized time-stamped ILC controller is introduced,

$$\underline{u}_{j+1} = \underline{u}_j + \underline{L} \underline{T}_{\bar{\tau}_j}^T \bar{e}_j \quad (14)$$

The advantage of this structure compared to (8) is that \underline{L} is identical for each $\bar{\tau} \in \mathcal{T}$. Hence, only $\underline{T}_{\bar{\tau}_j}$ varies, which can easily be constructed after the j -th iteration.

Exploiting Theorem 10, the following result is obtained for the ILC controller given by (14).

Theorem 11 (Decentralized ILC controller) *Consider the finite-time time-stamped ILC system (9) with desired output \underline{y}_d^h satisfying Assumption 3 and the ILC controller of the form (14). The sequence of control inputs $\{\underline{u}_j^l\}_{j \in \mathbb{N}}$ of (9) converges monotonically towards \underline{u}_d^l in the 2-norm, if and only if \underline{L} is given by*

$$\underline{L} := \underline{J}^{h,lT} D \quad (15)$$

with $D \in \mathbb{R}^{N_h \times N_h}$ a diagonal matrix with positive entries which satisfies the following linear matrix inequality (LMI)

$$2I_{N_l} - \underline{J}^{h,lT} D \underline{J}^{h,l} \succ 0. \quad (16)$$

Note that this design procedure is independent of the size of \mathcal{T} , since the procedure merely consists of finding a matrix D to satisfy the single condition (16). Hence, this method is considered to exhibit computational advantages compared to $\bar{\tau}_j$ specific design procedures, e.g., as in [11].

V. CONNECTION TO GRADIENT-DESCENT ILC

In this section, a connection is established between the ILC approach resulting from Theorem 11 and the gradient-descent ILC design method in [9], [10]. This connection allows for intuitive guidelines to design the matrix D , leading to contribution C3 of this paper.

A. Gradient-descent ILC

In gradient-descent ILC [9], [10] an iteration invariant ILC system is considered with finite-time description

$$\underline{e}_j = \underline{y}_d - \underline{J} \underline{u}_j. \quad (17)$$

The performance of the ILC algorithm is given by the cost function $\mathcal{J}(\underline{u}_{j+1}) = \underline{e}_{j+1}^T W_e \underline{e}_{j+1}$ with $W_e \succeq 0$ a user defined weighting matrix. The error at iteration $j+1$ can be written as $\underline{e}_{j+1} = \underline{e}_j + \underline{J}(\underline{u}_j - \underline{u}_{j+1})$ using (17). This leads to the following gradient of $\mathcal{J}(\underline{u}_{j+1})$ with respect to \underline{u}_{j+1} ,

$$\frac{\partial \mathcal{J}(\underline{u}_{j+1})}{\partial \underline{u}_{j+1}} = 2\underline{J}^T W_e \underline{J}(\underline{u}_{j+1} - \underline{u}_j) - 2\underline{J}^T W_e \underline{e}_j. \quad (18)$$

The learning update is given by choosing a control input in the steepest descent direction, i.e.,

$$\underline{u}_{j+1} = \underline{u}_j - \tilde{\epsilon} \left. \frac{\partial \mathcal{J}(\underline{u}_{j+1})}{\partial \underline{u}_{j+1}} \right|_{\underline{u}_{j+1}} = \underline{u}_j + \epsilon \underline{J}^T W_e \underline{e}_j, \quad (19)$$

with $\epsilon = 2\tilde{\epsilon} \in \mathbb{R}_{>0}$ the size of the step in the steepest descent direction. Choosing the step ϵ sufficiently small ensures that the cost function decays in each iteration, [9], [10], which leads to an increase in performance.

B. Connection to ILC approach in Theorem 11

The learning update for the ILC setup (9) with (14) and (15) is given by

$$\underline{u}_{j+1} = \underline{u}_j + \underline{J}^{h,lT} D \underline{T}_{\bar{\tau}_j}^T \underline{T}_{\bar{\tau}_j} \underline{e}_j. \quad (20)$$

Note that this learning update is equivalent to the update law (19), with $\epsilon W_e := D \underline{T}_{\bar{\tau}}^T \underline{T}_{\bar{\tau}} \succ 0$. Therefore, the learning update (20) at trial j is equivalent to a steepest descent update with cost function $\mathcal{J}_{\bar{\tau}_j}(\underline{u}_{j+1}) = \underline{e}_{j+1}^T D \underline{T}_{\bar{\tau}_j}^T \underline{T}_{\bar{\tau}_j} \underline{e}_{j+1}$. The matrix $\underline{T}_{\bar{\tau}}^T \underline{T}_{\bar{\tau}} \in \mathbb{R}^{N_h}$ is a diagonal matrix of the form

$$\underline{T}_{\bar{\tau}}^T \underline{T}_{\bar{\tau}} = \text{diag}(0, 0, 1, 0, 0, 0, 1, \dots, 0, 0, 1) \quad (21)$$

where the entries equal to 1 correspond to the available measurement points in the sequence $\bar{\tau}$.

The above observations allows the design of the matrix D to be equivalent to the intuitive design of a weighting matrix W_e which is extensively studied in literature [1]. By choosing $D = \alpha W_e$ with $W_e \in \mathbb{R}^{N_h \times N_h}$ a diagonal matrix with positive entries and a sufficiently small $\alpha \in \mathbb{R}_{>0}$ to satisfy (16) leads to monotonic convergence as in Definition 8.

VI. SIMULATION EXAMPLE

In this section, the decentralized ILC controller introduced in Section IV is applied to a mass-spring-damper system, with the following transfer function $J(s) = \frac{1}{ms^2 + cs + k}$ with mass $m = 1$ [kg], damping coefficient $c = 10$ [N·m/s], and spring constant $k = 100$ [N/m]. The position of the mass is measured by an incremental encoder with an accuracy of $5 \cdot 10^{-4}$ [m]. The sampling frequencies of the control input and encoder are, $h_l = 1 \cdot 10^{-2}$ [s] and $h_h = 1 \cdot 10^{-3}$ [s], respectively. The aim of this example is to find an input u^l such that the position of the mass follows the 4th order reference r , from which a scaled version is given by the dashed line in Fig. 4.

A traditional quantized ILC controller and a decentralized ILC controller (14) are designed using the finite-time description as discussed in Section III. The traditional quantized ILC controller exploits the counter data available at the sampling frequency of the control input, thereby introducing a quantization effect as discussed in Section II. This The traditional quantized ILC controller is given by (8) with $\underline{Q} = I_{N_l}$ and $\underline{L}_{\tau_0} = (\underline{J}^{l,l})^\dagger$. The decentralized ILC controller that exploits the exact data that is available at the time stamps, is determined using Theorem 11. For this application the error at each sample is considered to be of equal importance, this corresponds to a weighting filter $W_e = I_{N_h}$. Hence, the matrix D is designed as ϵI_{N_h} . The value of ϵ is chosen as $\epsilon = (\|\underline{J}^{h,lT} \underline{J}^{h,l}\|_{i2})^{-1}$ to satisfy Condition (16).

A. Simulation Results

In Fig. 5 the error norm $\|e_j^h\|_2$ when applying traditional quantized ILC and when applying the decentralized ILC controller. From Fig. 5 it is observed that the time-stamped ILC controller achieves higher performance, as the error norm $\|e_j^h\|_2$ of time-stamped ILC reaches a lower value compared to traditional quantized ILC. This can also be observed in Fig. 4 where the error of both ILC approaches after 500 trials is presented. It is also observed that the data

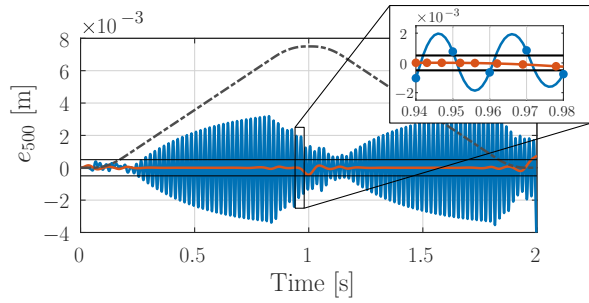


Fig. 4. Error e_{500} at trial 500 after applying traditional quantized ILC (—) and after applying the decentralized ILC controller of Theorem 11 (—). In the zoom the time-instances of the available error data are indicated by dots (● and ●). The quantization level is indicated by (—). The dashed line (---) depicts the reference scaled down by a factor 400.

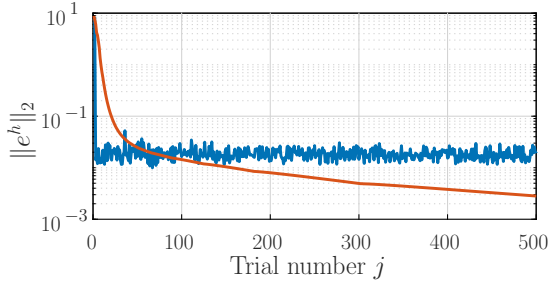


Fig. 5. Error norm $\|e_j^h\|_2$ when applying traditional quantized ILC (—) and when applying the decentralized ILC controller of Theorem 11 (—).

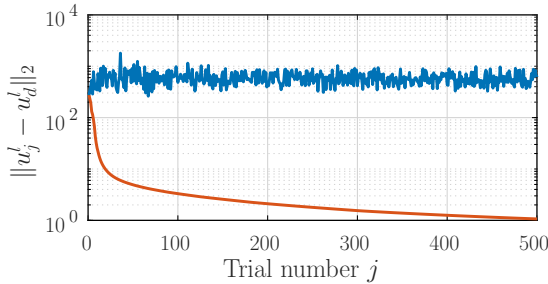


Fig. 6. Norm $\|u_j^l - u_d^l\|_2$ when applying traditional quantized ILC (—) and when applying the decentralized ILC controller of Theorem 11 (—).

used by the time-stamped ILC controller is non-equidistant in time. In Fig. 6 the monotonic convergence property of the sequence input signals in the 2-norm is evaluated for both ILC approaches. From 6 it is observed that when exploiting traditional quantized ILC convergence of the control input towards u_d^l is not achieved, where the control input of time-stamped ILC converges monotonically towards u_d^l .

VII. CONCLUSIONS

In this paper, a new framework for intermittent ILC is developed with provable monotonic convergence (in a suitably new definition), exploiting a single explicit ILC controller. This immediately allows large scale implementation of various relevant applications with intermittent observations, including systems with incremental encoders, and systems with networked or stealth attack issues. It is shown that due to the trial varying availability of the output, monotonic convergence in its standard definition cannot be obtained. A new definition for monotonic convergence for this type of systems

is introduced. A computationally efficient design procedure for an ILC algorithm that guarantees monotonic convergence is developed. A connection is established between the developed design procedure and the existing gradient-descent ILC approach leading to an intuitive design procedure. The developed design procedure is applied to a mass-spring-damper system, through numerical simulations monotonic convergence is illustrated.

REFERENCES

- [1] D. A. Bristow, M. Tharayil, and A. G. Alleyne, "A survey of iterative learning control," *IEEE Control Systems Magazine*, vol. 26, no. 3, pp. 96–114, 2006.
- [2] H. Ahn, Y. Chen, and K. L. Moore, "Iterative learning control: Brief survey and categorization," *IEEE Transactions on Systems, Man, and Cybernetics, Part C (Applications and Reviews)*, vol. 37, pp. 1099–1121, Nov 2007.
- [3] T. Oomen and C. R. Rojas, "Sparse iterative learning control with application to a wafer stage: Achieving performance, resource efficiency, and task flexibility," *Mechatronics*, vol. 47, pp. 134 – 147, 2017.
- [4] T. D. Son, G. Pipeleers, and J. Swevers, "Robust monotonic convergent iterative learning control," *IEEE Transactions on Automatic Control*, vol. 61, pp. 1063–1068, April 2016.
- [5] W. Paszke, E. Rogers, K. Gałkowski, and Z. Cai, "Robust finite frequency range iterative learning control design and experimental verification," *Control Engineering Practice*, vol. 21, no. 10, pp. 1310–1320, 2013.
- [6] N. Strijbosch, L. Blanken, and T. Oomen, "Frequency domain design of iterative learning control and repetitive control for complex motion systems," in *IEEJ International Workshop on Sensing, Actuation, Motion Control, and Optimization (SAMCON), Tokyo, Japan, 2018*.
- [7] N. Amann, D. Owens, and E. Rogers, "Iterative learning control for discrete-time-systems with exponential rate of convergence," *IEE Proc.-Control Theory & Appl.*, vol. 143, no. 2, pp. 217–224, 1996.
- [8] S. Gunnarsson and M. Norrlöf, "On the design of ILC algorithms using optimization," *Automatica*, vol. 37, no. 12, pp. 2011–2016, 2001.
- [9] D. Owens, J. Hatonen, and S. Daley, "Robust monotone gradient-based discrete-time iterative learning control," *International Journal of Robust and Nonlinear Control: IFAC-Affiliated Journal*, vol. 19, no. 6, pp. 634–661, 2009.
- [10] J. Bolder, S. Kleinendorst, and T. Oomen, "Data-driven multivariable ilc: enhanced performance by eliminating L and Q filters," *Int. Journal of Robust and Nonlinear Control*, vol. 28, no. 12, pp. 3728–3751.
- [11] N. Strijbosch and T. Oomen, "Beyond quantization in iterative learning control: Exploiting time-varying time-stamps," in *American Control Conference 2019, Philadelphia, USA, 2019* (Accepted for Publication).
- [12] H.-S. Ahn, K. L. Moore, and Y. Chen, "Discrete-time intermittent iterative learning controller with independent data dropouts," *IFAC Proceedings Volumes*, vol. 41, no. 2, pp. 12442 – 12447, 2008. 17th IFAC World Congress.
- [13] D. Shen and Y. Wang, "Iterative learning control for networked stochastic systems with random packet losses," *International Journal of Control*, vol. 88, no. 5, pp. 959–968, 2015.
- [14] G. Dan and H. Sandberg, "Stealth attacks and protection schemes for state estimators in power systems," in *2010 First IEEE International Conference on Smart Grid Communications*, pp. 214–219, Oct 2010.
- [15] B. Altn and R. G. Sanfelice, "Model predictive control under intermittent measurements due to computational constraints: Feasibility, stability, and robustness," in *2018 Annual American Control Conference (ACC)*, pp. 1418–1423, June 2018.
- [16] K. L. Barton and A. G. Alleyne, "A norm optimal approach to time-varying ILC with application to a multi-axis robotic testbed," *IEEE Trans. on Control Systems Technology*, vol. 19, pp. 166–180, Jan 2011.
- [17] J. A. Frueh and M. Q. Phan, "Linear quadratic optimal learning control (LQL)," *Int. Journal of Control*, vol. 73, no. 10, pp. 832–839, 2000.
- [18] M. Phan and R. Longman, "A mathematical theory of learning control for linear discrete multivariable systems," in *Astrodynamic Conference*, p. 4313, 1988.
- [19] K. Zhou, J. C. Doyle, K. Glover, *et al.*, *Robust and optimal control*, vol. 40. Prentice hall New Jersey, 1996.
- [20] J. C. Willems and J. W. Polderman, *Introduction to mathematical systems theory: a behavioral approach*, vol. 26. Springer Science & Business Media, 2013.
- [21] J. van de Wijdeven and O. Bosgra, "Residual vibration suppression using hankel iterative learning control," *International Journal of Robust and Nonlinear Control*, vol. 18, no. 10, pp. 1034–1051.